# Enthalpy and Entropy Decomposition of Free-Energy Changes for Side-Chain Conformations of Aspartic Acid and Asparagine in Acidic, Neutral, and Basic Aqueous Solutions

**Tomohiro Kimura,[†] Nobuyuki Matubayasi,[†] Hirofumi Sato,[‡] Fumio Hirata,[‡] and Masaru Nakahara*,[†]**

*Institute for Chemical Research, Kyoto University, Uji, Kyoto 611-0011, Japan, and Department of Theoretical Study, Institute for Molecular Science, Okazaki, Aichi 444-8585, Japan*

*Received: May 21, 2002; In Final Form: September 12, 2002*

Trans and gauche conformational equilibria in the side chains of aspartic acid (Asp) and asparagine (Asn) were investigated by measuring the vicinal spin−spin coupling constants of $^1$H NMR in acidic, neutral, and basic aqueous solutions over a wide range of temperature (5−90 °C). The standard free-energy changes $\Delta G^0$ were obtained for the trans to gauche conformational variations on the $C_\alpha-C_\beta$ bond with respect to the α-carboxyl group and the $\beta$-carboxyl group in Asp ($\beta$-amide in Asn) and were decomposed into enthalpic $\Delta H^0$ and entropic $-T\Delta S^0$ components. The hydration of ionic and polar groups in Asp competes against the large intramolecular electrostatic repulsion energy and stabilizes the gauche more than the trans conformer in correspondence to a larger degree of separation of positive and negative partial charges. In the neutral solutions, where both the carboxyl groups are negatively ionized, the hydration part even overwhelms the intramolecular repulsion and leads to a negative $\Delta H^0$. The fact that the hydration almost cancels the intramolecular electrostatic repulsion contradicts the widely accepted view that the trans preference in the conformational equilibrium is due to the intramolecular repulsion between α-$CO_2^-$ and $\beta$-$CO_2^-$ (or $\beta$-$CONH_2$).

## 1. Introduction

Understanding the conformational equilibrium in water is a very important issue in biochemistry and biophysics. Conceivable controlling factors for conformational equilibrium are electrostatic interactions, van der Waals interactions, hydrogen bonds, and hydrophobic effects.[1] Among these, intramolecular electrostatic interaction between ionized groups has been believed to control the ionized side-chain conformer distributions of amino acids and peptides in aqueous solution.[2−5] This is indeed the case in the gas phase. In aqueous solution, however, the simple interpretation must be scrutinized because of the presence of the hydration effect on the ionic and polar functional groups. Our purpose here is to gain insight into the role of hydration. The hydration effect is studied for aspartic acid (Asp) and asparagine (Asn), whose side-chain conformational equilibria at different ionization states can be inspected in detail by varying the pH (see the Asp and Asn structures in Figure 1a). Comprehensive measurements of the vicinal coupling constants in $^1$H NMR at dilute conditions will be performed by applying the three-staggered-state model shown in Figure 1b.[6]

For an understanding of the role of hydration of ionizable groups in the conformer free energies, it is of interest to carry out ab initio calculations for the molecule of interest in the gas phase. A determination of the energy change in the gas phase ($\Delta E^0_{gas}$) accompanying the conformational variation leads to the estimation of the hydration part of the free-energy change ($\Delta G^0_{hyd}$) given by

$$\Delta G^0_{hyd} = \Delta G^0 - \Delta E^0_{gas} \quad (1)$$

where $\Delta G^0$ is the experimentally obtainable overall free-energy change in solution. $\Delta G^0_{hyd}$ describes the effect of water on the conformational equilibrium and is the major target of the present study.

To elucidate the role of hydration, it is crucial to investigate separately the enthalpic ($\Delta H^0$) and entropic ($-T\Delta S^0$) compo-

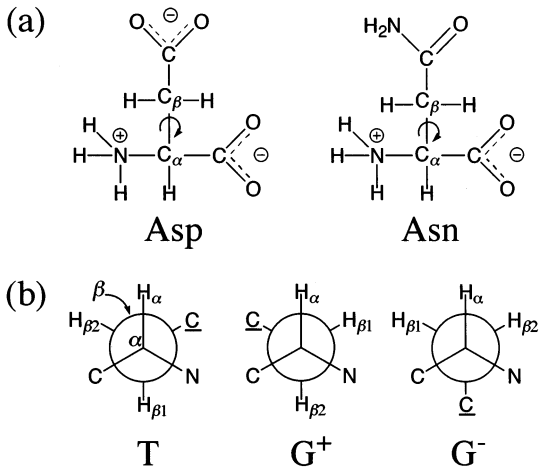


**Figure 1.** (a) Molecular structures of Asp and Asn with their ionization states in aqueous solution at neutral pH. The arrows represent the dihedral angles analyzed. (b) Staggered side-chain conformers of Asp or Asn with respect to the dihedral angles analyzed. C represents the $\beta$-carboxyl carbon for Asp or the $\beta$-amide carbon for Asn. N represents the α-amino nitrogen, and C represents the α-carboxyl carbon.

* To whom correspondence should be addressed. E-mail: nakahara@scl.kyoto-u.ac.jp. Phone: +81-774-38-3070. Fax: +81-774-38-3076.
[†] Kyoto University.
[‡] Institute for Molecular Science.

10.1021/jp021246o CCC: $22.00 
Published on Web 11/05/2002

nents of $\Delta G^0$ in aqueous solution. To the best of our knowledge, however, no attempt has ever been made to separate $\Delta H^0$ and $-T\Delta S^0$ for the side chains of amino acids and peptides in aqueous solution. Although the temperature effect on the conformer distributions was examined by NMR in a few papers,[3,7−9] the separation into $\Delta H^0$ and $-T\Delta S^0$ can be achieved only by studying the fine temperature effect. Only in the case of water-containing methanol solutions were $\Delta H^0$ and $-T\Delta S^0$ separated for the side chains of tryptophan (Trp) and histidine (His), and the compensation of $\Delta H^0$ and $-T\Delta S^0$ was referred to.[10,11]

To examine the reliability and limitations of the intramolecular electrostatic view for aqueous solution, we extract $\Delta H^0$ from $\Delta G^0$ because $\Delta H^0$ more directly reflects the electrostatic interaction energy, whereas other effects such as the excluded volume, in general, are also important in $\Delta G^0$. The experimentally observed $\Delta H^0$ value consists of the intramolecular term $\Delta E^0_{gas}$ and the hydration term $\Delta H^0_{hyd}$:

$$\Delta H^0 = \Delta E^0_{gas} + \Delta H^0_{hyd} \tag{2}$$

Thus, by combining the experimental results and theoretical calculations, the conformational energetics of the hydration and intramolecular effects can be separately discussed. Similarly, by separating $-T\Delta S^0$, we can discuss the hydration entropy $-T\Delta S^0_{hyd}$ since $-T\Delta S^0$ can be assumed here to be dominated by the hydration effect.

The organization of this paper is as follows. We introduce the basis for conformational analysis in section 2. In section 3, we describe the procedures for the NMR measurements and theoretical calculations. We present the ionization state and temperature dependence of the observed $J_{vic}$ in section 4.1 and the conformer distributions and $\Delta G^0$ in section 4.2. In section 4.3, we characterize the trends of the obtained values of $\Delta H^0$ and $-T\Delta S^0$ and discuss the role of hydration in determining the thermodynamic quantities. Concluding remarks will be given in section 5.

## 2. Basis for Conformational Analysis

**2.1. Conformer Probabilities.** A vicinal spin−spin coupling constant ($J_{vic}$) exhibits dihedral-angle dependence,[12] which allows us to examine the conformations of amino acids, peptides, and proteins for both the backbone and side chains.[6] For amino acid residues of ABX-type spin systems in $^1$H NMR, where the two $\beta$-protons couple strongly only with one α-proton, $J_{vic}$ between the α- and $\beta$-protons ($J_{\alpha\beta1}$ and $J_{\alpha\beta2}$) can be explicitly calculated by employing the reported procedure.[13] The experimentally observed $J_{\alpha\beta1}$ and $J_{\alpha\beta2}$ in solution are probability-weighted averages due to fast exchanges on the NMR time scale for the component conformers on the $C_\alpha-C_\beta$ bond shown in Figure 1b.[14] According to the three-staggered-state model, we express the observed $J_{\alpha\beta1}$ and $J_{\alpha\beta2}$ as

$$J_{\alpha\beta1} = P(\mathrm{T})J_t + P(\mathrm{G}^+)J_g + P(\mathrm{G}^-)J_g \tag{3a}$$

$$J_{\alpha\beta2} = P(\mathrm{T})J_g + P(\mathrm{G}^+)J_t + P(\mathrm{G}^-)J_g \tag{3b}$$

$$P(\mathrm{T}) + P(\mathrm{G}^+) + P(\mathrm{G}^-) = 1 \tag{3c}$$

where $P(\mathrm{T})$, $P(\mathrm{G}^+)$, and $P(\mathrm{G}^-)$ are the probabilities for conformers T, $G^+$, and $G^-$ defined in Figure 1b and $J_t$ and $J_g$ are the $J_{vic}$ values between the α- and $\beta$-protons in the trans and gauche conformers, respectively. In Figure 1b, the $\beta_1$-proton takes the trans conformation to the α-proton in conformer T and the gauche conformation in conformers $G^+$ and $G^-$. We name the conformers according to the method used above to focus on the dihedral angle for the α-carboxyl and $\beta$-carboxyl carbons in Asp ($\beta$-amide in Asn); T represents trans, whereas $G^+$ and $G^-$, gauche. The conformer distribution of the side chain can be evaluated by solving eqs 3a−3c. We also mention that the NMR signals from the two $\beta$-protons were assigned to $\beta_1$ and $\beta_2$ on the basis of the deuterium labeling experiment.[4]

To determine the probabilities in the rapid-exchange mechanism from the observed $J_{\alpha\beta1}$ and $J_{\alpha\beta2}$, we need a set of parameters $J_t$ and $J_g$. It is known that the parameters depend on the electronegativity of the substituent.[15] An appropriate set including the substituent effect for amino acids was developed by Pachler[14] and has been used widely.[6] In this work, the side-chain conformer probabilities of Asp and Asn amino acids were estimated by using Pachler's parameter set.

It was reported that the substituent effect on $J_{vic}$ depends on the relative configuration of the substituent with regard to the coupling nuclei,[16] and Feeney's parameter set takes account of this effect in parameters $J_t$ and $J_g$.[17] In this paper, we report the results from Pachler's parameter set because it was confirmed that the examination with the two parameter sets of Pachler and Feeney provides identical conclusions on the distribution trend.

**2.2. Standard Thermodynamic Quantities.** The equilibrium constant ($K_{x/T}$) between conformers T and x is represented by

$$K_{x/T} = \frac{P(\mathrm{x})}{P(\mathrm{T})} \tag{4}$$

where $P(\mathrm{T})$ and $P(\mathrm{x})$ are the probabilities of conformers T and x, respectively (x denotes either conformer $G^+$ or $G^-$). Conformer T is chosen as the reference since the large probability of this conformer is of particular interest in view of the role of intramolecular electrostatic interaction between α-$CO_2^-$ and $\beta$-$CO_2^-$ in Asp ($\beta$-$CONH_2$ in Asn). The $K_{x/T}$ value is then related to the standard free-energy change $\Delta G^0(\mathrm{T} \rightarrow \mathrm{x})$ from T to x through the thermodynamic relation

$$\ln K_{x/T} = -\frac{\Delta G^0(\mathrm{T} \rightarrow \mathrm{x})}{RT} \tag{5}$$

where the $T$ is the absolute temperature (K) and $R$ is the gas constant (kJ mol$^{-1}$ K$^{-1}$). The standard enthalpy change $\Delta H^0(\mathrm{T} \rightarrow \mathrm{x})$ is obtained from the van't Hoff equation, and the standard entropy change $-T\Delta S^0(\mathrm{T} \rightarrow \mathrm{x})$ is simply given by $\Delta G^0(\mathrm{T} \rightarrow \mathrm{x}) - \Delta H^0(\mathrm{T} \rightarrow \mathrm{x})$.

## 3. Methods

**3.1. Materials.** L-Aspartic acid (Asp) monopotassium salt (GR grade) was purchased from Nakalai, and L-asparagine (Asn) was from Sigma. Both of these materials were used without further purification. Deuterium oxide solvent ($D_2O$; 99.90% D) was purchased from Euriso-top. $D_2O$ solutions of DCl (18 wt %) and NaOD (40 wt %) used to control the solution pD were from Aldrich.

Aqueous solutions of Asp and Asn were prepared at 20 mM. At this concentration, we can neglect the effect of intermolecular interactions among the solute molecules on the conformer distributions. To vary the solute ionization state, the aqueous solutions were prepared at three different pD conditions (see the pD values in Table 1). The pD values were obtained by adding 0.4 unit to the pH meter (HORIBA D-21) readings.[18]

**3.2. $^1$H NMR Measurements.** $^1$H NMR measurements of aqueous solutions of Asp and Asn were carried out on a 270-MHz spectrometer (JEOL JNM-EX270) equipped with probes

**TABLE 1: Observed Spin−Spin Coupling Constants (Hz) among the α- and β-Protons of Asp and Asn Amino Acids in Acidic, Neutral, and Basic Aqueous Solutions at Various Temperatures**

| amino acid | solution condition | $J$ | temperature/°C | | | | | | | | |
|---|---|---|---|---|---|---|---|---|---|---|---|
| | | | 10 | 20 | 30 | 40 | 50 | 60 | 70 | 80 | 90 |
| Asp | acidic | $J_{\alpha\beta1}$ | 6.28 ± 0.01 | 6.33 ± 0.00 | 6.37 ± 0.05 | 6.45 ± 0.01 | [a] | [a] | [a] | [a] | [a] |
| | (pD = 0.9) | $J_{\alpha\beta2}$ | 4.18 ± 0.01 | 4.27 ± 0.01 | 4.32 ± 0.05 | 4.34 ± 0.02 | [a] | [a] | [a] | [a] | [a] |
| | | $J_{\beta1\beta2}$ | 18.37 ± 0.00 | 18.36 ± 0.01 | 18.36 ± 0.01 | 18.33 ± 0.01 | [a] | [a] | [a] | [a] | [a] |
| | neutral | $J_{\alpha\beta1}$ | 9.07 ± 0.03 | 9.08 ± 0.02 | 9.10 ± 0.01 | 9.13 ± 0.00 | 9.17 ± 0.01 | 9.21 ± 0.00 | 9.25 ± 0.01 | 9.28 ± 0.01 | 9.31 ± 0.01 |
| | (pD = 7.3) | $J_{\alpha\beta2}$ | 3.49 ± 0.03 | 3.54 ± 0.01 | 3.58 ± 0.02 | 3.62 ± 0.01 | 3.64 ± 0.01 | 3.64 ± 0.00 | 3.67 ± 0.01 | 3.68 ± 0.01 | 3.68 ± 0.02 |
| | | $J_{\beta1\beta2}$ | 17.52 ± 0.04 | 17.50 ± 0.01 | 17.47 ± 0.01 | 17.42 ± 0.01 | 17.39 ± 0.01 | 17.34 ± 0.01 | 17.30 ± 0.01 | 17.27 ± 0.01 | 17.21 ± 0.03 |
| | basic | $J_{\alpha\beta1}$ | 10.17 ± 0.01 | 10.12 ± 0.01 | 10.08 ± 0.00 | 10.02 ± 0.01 | 9.97 ± 0.00 | 9.95 ± 0.01 | 9.88 ± 0.02 | 9.84 ± 0.00 | 9.81 ± 0.01 |
| | (pD = 13.8) | $J_{\alpha\beta2}$ | 3.59 ± 0.00 | 3.63 ± 0.01 | 3.64 ± 0.01 | 3.70 ± 0.01 | 3.72 ± 0.00 | 3.74 ± 0.00 | 3.78 ± 0.00 | 3.79 ± 0.00 | 3.80 ± 0.01 |
| | | $J_{\beta1\beta2}$ | 15.37 ± 0.00 | 15.33 ± 0.01 | 15.30 ± 0.00 | 15.27 ± 0.00 | 15.24 ± 0.00 | 15.21 ± 0.00 | 15.18 ± 0.00 | 15.16 ± 0.00 | 15.13 ± 0.00 |
| Asn | acidic | $J_{\alpha\beta1}$ | 6.23 ± 0.02 | 6.36 ± 0.03 | 6.55 ± 0.02 | [a] | [a] | [a] | [a] | [a] | [a] |
| | (pD = 1.2) | $J_{\alpha\beta2}$ | 4.43 ± 0.03 | 4.44 ± 0.03 | 4.31 ± 0.03 | [a] | [a] | [a] | [a] | [a] | [a] |
| | | $J_{\beta1\beta2}$ | 17.37 ± 0.01 | 17.45 ± 0.01 | 17.44 ± 0.01 | [a] | [a] | [a] | [a] | [a] | [a] |
| | neutral | $J_{\alpha\beta1}$ | 7.93 ± 0.01 | 7.95 ± 0.01 | 7.96 ± 0.01 | 7.98 ± 0.01 | 8.00 ± 0.01 | 8.03 ± 0.01 | 8.03 ± 0.01 | 8.06 ± 0.01 | 8.07 ± 0.01 |
| | (pD = 7.7) | $J_{\alpha\beta2}$ | 4.05 ± 0.02 | 4.08 ± 0.00 | 4.12 ± 0.02 | 4.13 ± 0.01 | 4.14 ± 0.02 | 4.16 ± 0.01 | 4.18 ± 0.01 | 4.18 ± 0.02 | 4.19 ± 0.03 |
| | | $J_{\beta1\beta2}$ | 16.92 ± 0.01 | 16.90 ± 0.00 | 16.89 ± 0.00 | 16.88 ± 0.01 | 16.86 ± 0.01 | 16.85 ± 0.01 | 16.83 ± 0.01 | 16.82 ± 0.02 | 16.84 ± 0.01 |
| | basic | $J_{\alpha\beta1}$ | 9.18 ± 0.02 | 9.11 ± 0.01 | 9.05 ± 0.01 | 8.98 ± 0.01 | 8.90 ± 0.00 | 8.83 ± 0.00 | 8.78 ± 0.01 | 8.71 ± 0.00 | 8.65 ± 0.01 |
| | (pD = 12.6) | $J_{\alpha\beta2}$ | 4.63 ± 0.02 | 4.68 ± 0.01 | 4.71 ± 0.01 | 4.74 ± 0.01 | 4.76 ± 0.00 | 4.79 ± 0.01 | 4.80 ± 0.00 | 4.83 ± 0.01 | 4.84 ± 0.02 |
| | | $J_{\beta1\beta2}$ | 14.72 ± 0.00 | 14.76 ± 0.01 | 14.77 ± 0.00 | 14.79 ± 0.00 | 14.81 ± 0.00 | 14.83 ± 0.00 | 14.84 ± 0.01 | 14.86 ± 0.01 | 14.88 ± 0.01 |

[a] Values could not be obtained because of signal overlap.

for 5- or 10-mm o.d. sample tubes. Free-induction decay (FID) signals were accumulated 8 to 64 times. The digital frequency resolution was set to 0.01 Hz.

The temperature effect was examined at an interval of 10 °C from 10 to 90 °C except at the acidic pD, where the examination was done at an interval of 5 °C from 5 to 40 °C for Asp and from 5 to 30 °C for Asn. At the acidic pD, we restricted the temperature range because of the signal overlap at the higher temperatures. The temperature uncertainties were ±0.1 °C. The FID signals were obtained more than 30 min after a temperature change. At each temperature, the measurement was repeated two or three times.

**3.3. Calculations of Conformer Energies and Effective Polarities.** Calculations of the electronic structure and effective charges $q_j$ on the constituent atoms $j$ of the side-chain conformers of Asp in the gas phase were carried out at the ab initio Hartree−Fock level of approximation. The Gaussian basis set, (9s, 5p)/[3s, 2p], for the double-ζ qualities of Slater-type orbitals was used with the single d-polarization functions (exponents 0.75 for carbon, 0.80 for nitrogen, and 0.85 for oxygen).[19] The consideration of electron correlation by the second-order perturbative Møller−Plesset (MP2) formalism or the use of a larger basis set of 6-311G(d,p) affected the conformational energy change by less than ∼4 kJ mol$^{-1}$. The effective charges in the solute molecule were determined by the electrostatic potential (ESP) fitting procedure.

The geometry optimizations were carried out with the dihedral angles constrained to those shown in Figure 1b. The ionization states calculated correspond to those at the experimental pD conditions. In the optimization, the orientation of the neutral α-carboxyl group (or β-carboxyl group) was chosen so that the carbonyl oxygen was closer than the hydroxyl oxygen to the α-ammonium group (or α-carbon). The orientation of hydroxyl part of the carboxyl group was also chosen so that the hydroxyl hydrogen was closer to the carbonyl group. It was confirmed that the alternative orientations lead to an increase in the conformational energy. The conformation of the neutral amino group was optimized to ensure the energy minimum. All of the computations were performed with the program package GAMESS.[20]

According to thorough ab initio investigations of the gas-phase potential energy surface of glycine, there is general agreement that α-amino acids in the gas phase are energetically more favorable in the neutral form than in the zwitterionic form.[21,22] However, for our present purpose of discussing the hydration effect on the charged species, it is useful to determine the ab initio gas-phase energy of the zwitterionic form, which often appears as a local minimum for certain basis sets including ours.[23]

To see the effect of the hydration part of the free energy change $\Delta G^0_{hyd}$ given by eq 1, it is of interest to seek the correlation of the $\Delta G^0_{hyd}$ value with some index for the solute−solvent interactions. Since the molecules of interest in the present study carry both positive and negative charges, we introduce the effective polarity $\mu^\dagger$ as an empirical index with which to characterize the strength of the solute−solvent interaction. $\mu^\dagger$ is defined as the dipole moment with its coordinate origin positioned at the charge center $\vec{r}_e = \sum_j |q_j| \vec{r}_j / \sum_j |q_j|$:

$$\mu^\dagger = \sum_j q_j (\vec{r}_j - \vec{r}_e) = \frac{2Q^+Q^-}{Q^+ + Q^-} l \qquad (6)$$

where $\vec{r}_j$ represents the position of a partial charge $q_j$, $2Q^+Q^-/(Q^+ + Q^-)$ is the harmonic mean of the sum of the positive charges $Q^+ = \sum_{q_j>0} q_j$ and the sum of the negative charges $Q^- = \sum_{q_j<0} |q_j|$, and $l$ is the distance between the centers of positive and negative charges. Our definition of $\mu^\dagger$ precludes the ambiguity of the coordinate origin involved in the definition of the dipole moment for charged species. When the molecule is neutral and $Q^+ = Q^-$ ($\equiv Q$), $\mu^\dagger$ reduces to the conventional dipole moment $\mu$ ($= Ql$). Replacement of the harmonic mean with the geometric or arithmetic mean gives the conformer polarity index, which is larger than $\mu^\dagger$, according to

$$\frac{2Q^+Q^-}{Q^+ + Q^-} \le \sqrt{Q^+Q^-} \le \frac{Q^+ + Q^-}{2} \qquad (7)$$

It was confirmed that the differences due to the choice of the mean are small enough for our discussion on the hydration effect. Among the conformers at the same ionization state, the variation of $Q^+$ or $Q^-$ is less than 10% whereas that of $l$ is ∼100%. Thus, the conformer dependence of $\mu^\dagger$ is dominated

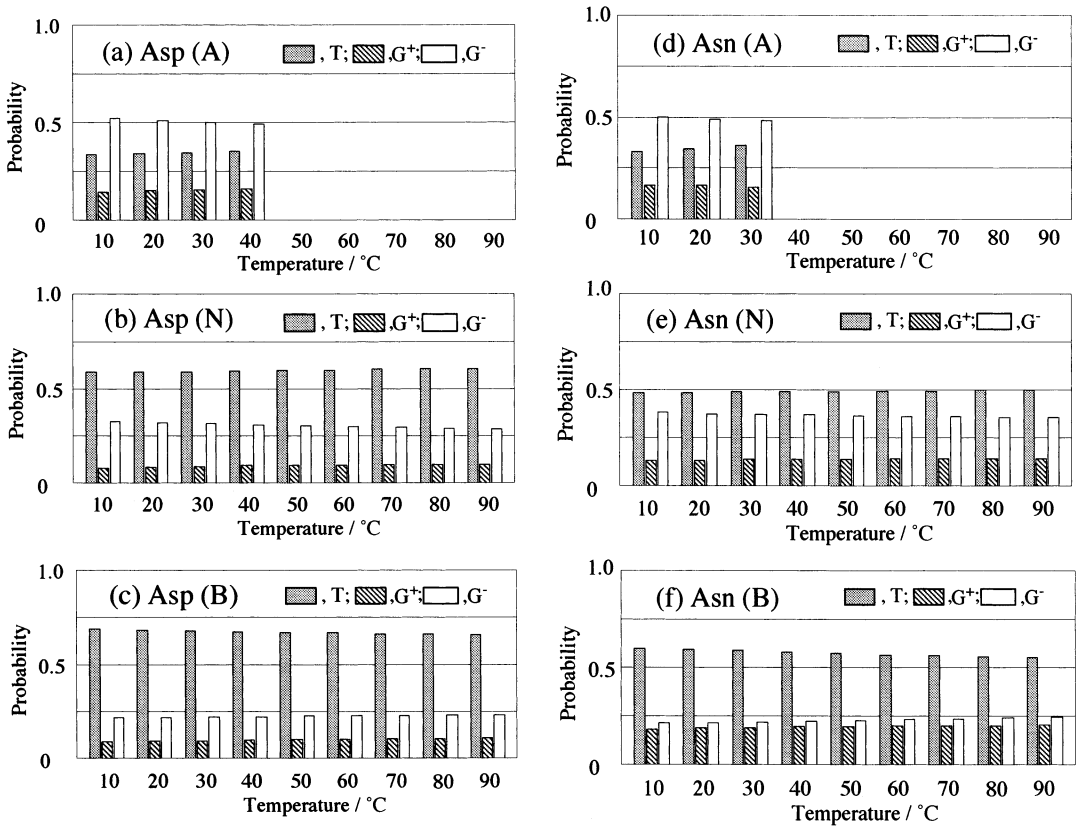


**Figure 2.** Temperature dependence of the probabilities of side-chain conformers T, $G^+$, and $G^-$ in Figure 1b. (a) Asp at acidic pD = 0.9 (A); (b) Asp at neutral pD = 7.3 (N); (c) Asp at basic pD = 13.8 (B); (d) Asn at acidic pD = 1.2 (A); (e) Asn at neutral pD = 7.7 (N); and (f) Asn at basic pD = 12.6 (B).

by the variations of *l*. In other words, $\mu^\dagger$ characterizes the charge separation in each conformer.

## 4. Results and Discussion

**4.1. Proton Coupling Constants.** In the $^1$H NMR spectra of Asp and Asn aqueous solutions, the signals from the single α-proton involve four peaks, and those from the two *β*-protons involve eight peaks, irrespective of the ionization state (pD) and temperature. These typical ABX-type signals indicate unequal probabilities of rapidly exchanging side-chain conformers on the α−*β* bond. By taking the frequency differences among the peaks, we can determine the two vicinal coupling constants ($J_{vic}$) between the α- and *β*-protons ($J_{\alpha\beta1}$ and $J_{\alpha\beta2}$).[13]

The $J_{\alpha\beta1}$ and $J_{\alpha\beta2}$ values obtained for Asp and Asn at acidic, neutral, and basic pD in the temperature range of 10−90 °C are listed in Table 1. At the acidic pD, the amino group is positively charged, and the carboxyl groups are neutral. At the neutral pD, the amino group is positively charged, and the carboxyl groups are negatively charged (cf. Figure 1a). At the basic pD, the amino group is neutral, and the carboxyl groups are negatively charged. The difference between $J_{\alpha\beta1}$ and $J_{\alpha\beta2}$ at each temperature becomes larger for both Asp and Asn when the carboxyl groups ionize at neutral and basic pD. In contrast, the ionization effect of the amino group on $J_{\alpha\beta1}$ and $J_{\alpha\beta2}$ is less significant than that of the carboxyl groups.

The temperature effect on $J_{\alpha\beta1}$ and $J_{\alpha\beta2}$ is minute over the temperature range examined. This means that as shown in Table 1, high precision is necessary for the determination of the thermodynamic quantities for the conformer equilibrium.

**4.2. Conformer Distribution and Free-Energy Changes.** *4.2.1. Conformer Distribution.* In this section, we show the ionization-state and temperature dependencies of the side-chain conformer distributions on the $C_\alpha-C_\beta$ bonds of Asp and Asn in aqueous solution.

**TABLE 2: Changes in the Standard Energy $\Delta E^0$ (kJ mol$^{-1}$) Accompanying Trans−Gauche Conformational Variations of Asp in the Gas Phase**

| ionization state | T → $G^+$ | T → $G^-$ |
|---|---|---|
| acidic pH | 49.0 | 3.3 |
| neutral pH | [a] | 32.3 |
| basic pH | 46.1 | 20.9 |

[a] Value could not be calculated because of the hydrogen transfer from α-$NH_3^+$ to α-$CO_2^-$ in the optimization.

How the conformer distribution depends on the pD and the temperature is illustrated for Asp in Figure 2a−c and for Asn in Figure 2d−f. At each temperature, the distributions depend markedly on the ionization state of the carboxyl groups, whereas the dependence is relatively small for the amino group. Consider, for example, Asp at 30 °C. At the basic and neutral conditions, where the carboxyl groups are ionized, *P*(T) of Asp amounts to 0.69 and 0.59, respectively. In contrast, at the acidic condition, where the carboxyl groups are not ionized, *P*(T) is only 0.34 and is about half the value of *P*(T) at the basic and neutral conditions. For Asn, *P*(T) is equal to 0.59, 0.49, and 0.36 at the basic, neutral, and acidic pD conditions, respectively. In this case, although the effect of the ionization of the carboxyl groups is smaller, the trend is the same as that for Asp. The above trend in the distributions at room temperature is in agreement with that in the literature, within the probability of $P \leq 0.07$.[2,4] As can be seen in Figure 2, the small conformational changes due to temperature variations are in remarkable contrast with the changes due to pD (ionization state).

*4.2.2. Hydration Free Energies.* In previous works,[2,4] the *P*(T) enhancements of the carboxyl ionization are ascribed to

**TABLE 3: Experimentally Observed Changes in the Standard Free Energy $\Delta G^0$, Enthalpy $\Delta H^0$, and Entropy $-T\Delta S^0$ (kJ mol$^{-1}$) Accompanying Trans−Gauche Conformational Variations of Asp and Asn in Aqueous Solutions at 30 °C**

| amino acid | pD | | T → G$^+$ | T → G$^-$ | amino acid | pD | | T → G$^+$ | T → G$^-$ |
|---|---|---|---|---|---|---|---|---|---|
| Asp | 0.9 | $\Delta G^0$ | 2.0 ± 0.1 | −1.0 ± 0.1 | Asn | 1.2 | $\Delta G^0$ | 2.1 ± 0.1 | −0.8 ± 0.0 |
| | | $\Delta H^0$ | 1.0 ± 0.3 | −2.8 ± 0.0 | | | $\Delta H^0$ | −3.5 ± 0.6 | −3.9 ± 0.2 |
| | | $-T\Delta S^0$ | 1.0 ± 0.4 | 1.8 ± 0.1 | | | $-T\Delta S^0$ | 5.6 ± 0.7 | 3.1 ± 0.2 |
| | 7.3 | $\Delta G^0$ | 4.8 ± 0.0 | 1.6 ± 0.0 | | 7.7 | $\Delta G^0$ | 3.2 ± 0.1 | 0.7 ± 0.0 |
| | | $\Delta H^0$ | 1.7 ± 0.2 | −1.9 ± 0.1 | | | $\Delta H^0$ | 0.7 ± 0.1 | −1.0 ± 0.1 |
| | | $-T\Delta S^0$ | 3.1 ± 0.2 | 3.5 ± 0.1 | | | $-T\Delta S^0$ | 2.5 ± 0.1 | 1.7 ± 0.1 |
| | 13.8 | $\Delta G^0$ | 5.0 ± 0.1 | 2.8 ± 0.0 | | 12.6 | $\Delta G^0$ | 2.8 ± 0.0 | 2.5 ± 0.0 |
| | | $\Delta H^0$ | 2.7 ± 0.0 | 1.2 ± 0.1 | | | $\Delta H^0$ | 1.9 ± 0.2 | 2.3 ± 0.1 |
| | | $-T\Delta S^0$ | 2.3 ± 0.1 | 1.6 ± 0.1 | | | $-T\Delta S^0$ | 0.9 ± 0.2 | 0.2 ± 0.1 |

the intramolecular electrostatic repulsion. To elucidate the effect of solvent quantitatively, however, it is necessary to determine the conformational energy change in the gas phase ($\Delta E^0_{gas}$) since we can isolate the hydration part of the conformational free-energy change ($\Delta G^0_{hyd}$) according to eq 1.

Results of ab initio calculations of $\Delta E^0_{gas}$ for the Asp conformers are summarized in Table 2. The energy change $\Delta E^0_{gas}$ accompanying the trans to gauche conformational variation increases drastically by more than 1 order of magnitude upon the carboxyl ionization because of the increased electrostatic interactions between the carboxyl groups.[24] For example, $\Delta E^0_{gas}$(T → G$^-$) is 3.3 and 32.3 kJ mol$^{-1}$ when the carboxyl groups are neutral and ionized, respectively. Therefore, if the intramolecular electrostatic interaction is dominant in determining the pD dependence of the conformational equilibrium, then the probabilities in solution at different pD values could not be comparable to each other as shown in Figure 2.

Table 3 shows the experimentally determined changes $\Delta G^0$ of the standard free energy upon the conformational variation in aqueous solution. According to Table 3, the variation of the $\Delta G^0$(T → G$^+$, G$^-$) values with the carboxyl ionization is much smaller than that of the corresponding $\Delta E^0_{gas}$(T → G$^+$, G$^-$). This implies that the hydration effect $\Delta G^0_{hyd}$ almost cancels $\Delta E^0_{gas}$ for ionic groups. For example, $\Delta G^0_{hyd}$(T → G$^-$) in aqueous solution is −4.3 and −30.7 kJ mol$^{-1}$ when the carboxyl groups are neutral and ionized, respectively. For the ionized carboxyl groups, the free-energy change $\Delta G^0$(T → G$^-$) in aqueous solution is thus ∼$^1/_{20}$ of the energy change $\Delta E^0_{gas}$(T → G$^-$) in the gas phase. In other words, when the carboxyl groups are ionized, the hydration stabilizes the gauche conformer more than the trans, thus competing against the strong intramolecular electrostatic repulsion between the ionized carboxyl groups.

*4.2.3. Correlation between Changes in Hydration Free Energy and in Effective Polarity.* To provide insight into the hydration effect, we examine the effective polarities $\mu^\dagger$ defined in eq 6 as an index of the degree of separation of positive and negative partial charges within the conformer. A larger $\mu^\dagger$ is expected to cause stronger hydration and reduce the free energy of the conformer. The calculated $\mu^\dagger$ values are summarized in Table 4.

Figure 3 plots $-\Delta G^0_{hyd}$ against the conformational change $\Delta\mu^\dagger$ of the effective polarity. We see that $-\Delta G^0_{hyd}$ increases in trend with $\Delta\mu^\dagger$. It is thus concluded that the magnitude of $\mu^\dagger$ is correlated to the degree of conformer stabilization through the hydration effect.

**4.3. Conformer Enthalpies and Entropies.** *4.3.1. Observations.* In Figure 4a−c, we plot the side-chain conformational equilibrium constants ln $K_{x/T}$ against the inverse temperature $1/T$ for Asp and Asn in acidic, neutral, and basic aqueous solutions. The plots show a good linear relationship over the

**TABLE 4: Effective Polarities $\mu^\dagger$ (D) of Asp in the Gas Phase for Side-Chain Conformers T, G$^+$, and G$^-$ in Figure 1b[a]**

| amino acid | ionization state | conformer | $\mu^\dagger$ |
|---|---|---|---|
| Asp | acidic pH | T | 1.6 |
| | | G$^+$ | 6.8 |
| | | G$^-$ | 5.4 |
| | neutral pH | T | 7.1 |
| | | G$^+$ | [b] |
| | | G$^-$ | 11.2 |
| | basic pH | T | 5.3 |
| | | G$^+$ | 9.1 |
| | | G$^-$ | 6.6 |

[a] The definition of $\mu^\dagger$ is described in eq 6 in Section 3.3. [b] The value could not be calculated because of the hydrogen transfer from α-$NH_3^+$ to α-$CO_2^-$ in the optimization.

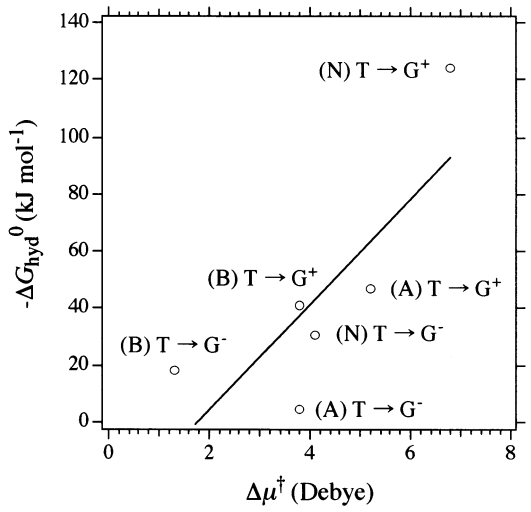


**Figure 3.** $-\Delta G^0_{hyd}$ against $\Delta\mu^\dagger$ for Asp at acidic (A), neutral (N), and basic (B) pD conditions. $\Delta\mu^\dagger$ and $\Delta E^0_{gas}$ were determined by ab initio calculations except for T → G$^+$ at (N), where $\Delta E^0_{gas}$ was calculated by the MM2 force field and $\mu^\dagger$ for G$^+$ was from the semiempirical AM1 calculation; see ref 24. The line represents the regression line obtained by the least-squares analysis.

measured temperature range. This means that $\Delta H^0$(T → x) is temperature-independent over the present experimental range. Table 3 lists $\Delta G^0$(T → x), $\Delta H^0$(T → x), and $-T\Delta S^0$(T → x) values at 30 °C. In Figure 5, we diagrammatically illustrate the $\Delta G^0$, $\Delta H^0$, and $-T\Delta S^0$ values reported in Table 3 by taking conformer T as the reference state.

In the $H^0$ diagram, the enthalpies of gauche conformers G$^+$ and G$^-$ relative to that of trans conformer T become larger when the carboxyl groups are ionized. This trend is common to Asp and Asn. As shown in the previous section, the carboxyl ionization of Asp in the gas phase increases the energies of the

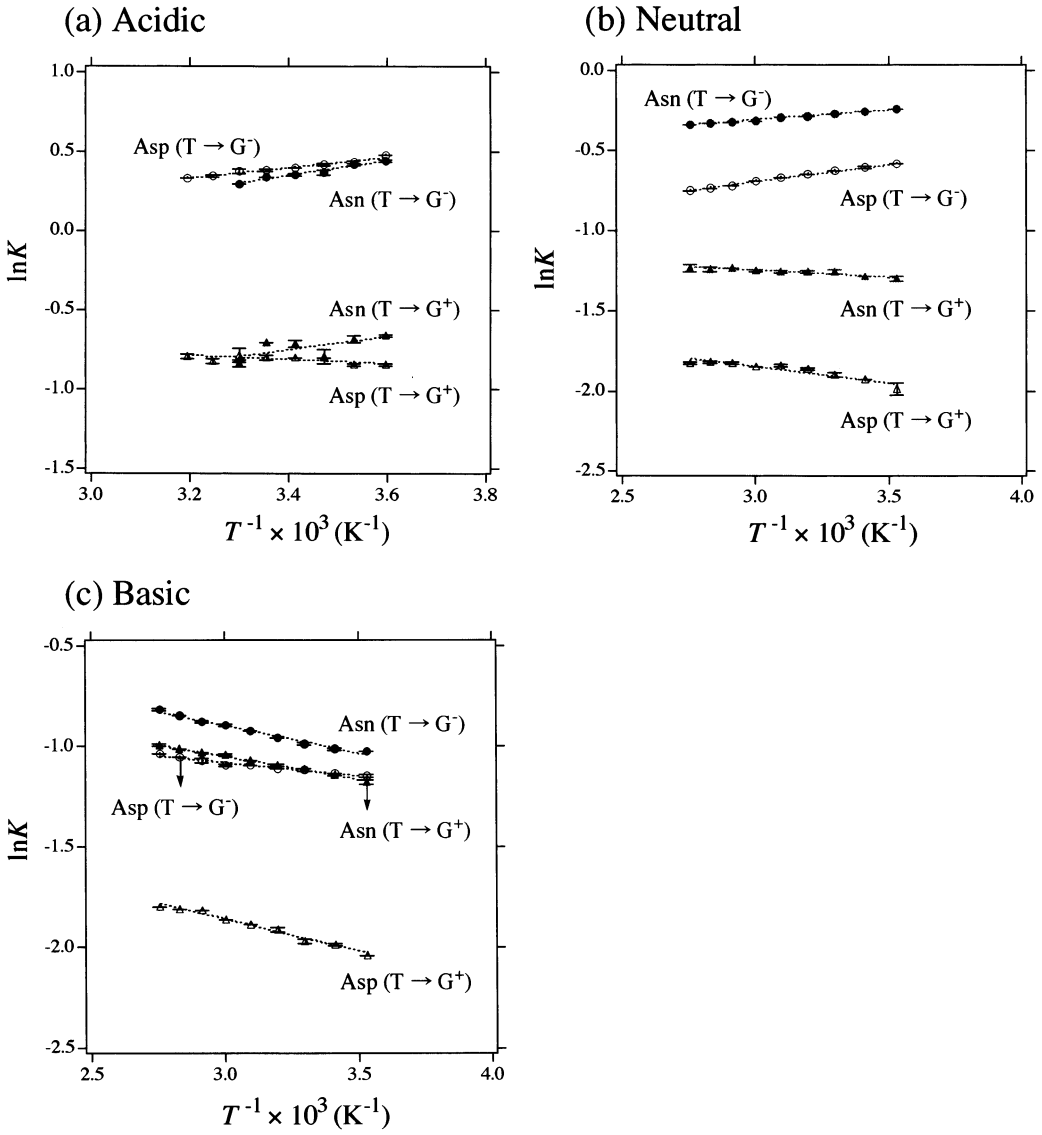


**Figure 4.** ln *K* against 1/*T* for the side-chain conformational equilibria of Asp and Asn; for the definition of *K*, see eq 4. (a) In acidic water (A) at pD = 0.9 for Asp and at pD = 1.2 for Asn; (b) in neutral water (N) at pD = 7.3 for Asp and at pD = 7.7 for Asn; and (c) in basic water (B) at pD = 13.8 for Asp and at pD = 12.6 for Asn.

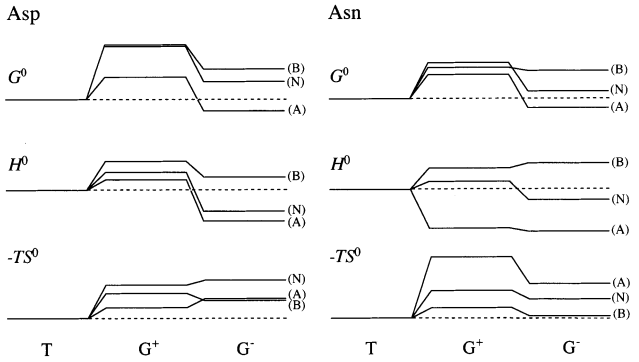


**Figure 5.** Diagrams of $G^0$, $H^0$, and $-TS^0$ at 30 °C for conformers T, G$^+$, and G$^-$ of Asp and Asn in acidic (A), neutral (N), and basic (B) aqueous solutions. Conformer T is taken as the reference.

gauche conformers much more than that of the trans conformer because of strong electrostatic repulsion between α-$CO_2^-$ and β-$CO_2^-$ (see Table 2 and ref 24). In contrast to those in the gas phase, the observed enthalpy trends in aqueous solution show no drastic changes upon carboxyl ionization for both Asp and Asn. Therefore, the hydration reduces the enthalpies of the gauche conformers more than that of the trans, opposing the steep increase in the intramolecular electrostatic repulsion energy due to the ionization of the carboxyl groups. The enthalpy reduction in the gauche conformers is attributed to the stronger hydration of these conformers. In particular, as seen in Figure 5, we observe a smaller total enthalpy of gauche conformer G$^-$ than that of trans conformer T at neutral pD, despite the presence of the repulsion between α-$CO_2^-$ and β-$CO_2^-$. This is an extreme case, where the effect of the hydration enthalpy overwhelms that of the intramolecular electrostatic repulsion energy.

Compare the $H^0$ diagram at the neutral and basic pD conditions, where the carboxyl groups are ionized with the amino group ionized and neutral, respectively. $\Delta H^0$ for the transformation from the trans to the gauche conformer is larger at the basic pD than at the neutral pD, whereas the corresponding $\Delta E^0_{gas}$ is larger at the neutral pD (cf. Table 2 and ref 24). This indicates that the changes in hydration enthalpy are smaller when the solution is basic and the amino group is neutral. As discussed in the following section, the smaller changes in hydration enthalpy are correlated with smaller changes in the conformer effective polarity $\mu^\dagger$.

We can illustrate more clearly the hydration effect using the entropy changes. What is most outstanding in the $-TS^0$ diagram is that in both Asp and Asn, the entropy of the gauche conformers is smaller than that of the trans. This trend is common to acidic, neutral, and basic aqueous solutions. The smaller entropy of the gauche conformers is attributed to the more intensive hydration, which restricts the freedom of hydrating water molecules.

*4.3.2. Correlation between Changes in Hydration Enthalpy and Entropy and in Effective Polarity.* The trends of the effective polarities for Asp conformers in Table 4 are summarized as follows. The $\mu^\dagger$ of trans conformer T is relatively small at any ionization state, ranging from 2 to 7 D. Conformational polarity changes $\Delta\mu^\dagger(T \rightarrow G^+, G^-)$ increase upon ionization of the carboxyl groups and upon ionization of the amino group.[26]

The observable conformational enthalpy change $\Delta H^0$ consists of the intramolecular part $\Delta E^0_{gas}$ and the hydration part $\Delta H^0_{hyd}$, as shown in eq 2. Although the examination of the correlation between $\Delta H^0_{hyd}$ and $\Delta\mu^\dagger$ provides insight into the enthalpic effect of hydration, a careful examination of $\Delta H^0$ provides qualitative information about the correlation without resorting to the $\Delta E^0_{gas}$ values. For example, $\Delta\mu^\dagger(T \rightarrow G^-)$ in Asp increases markedly on the ionization of the amino group, whereas the effect of intramolecular electrostatic repulsion between the ionized carboxyl groups is not changed by the ionization. It is expected, therefore, that $\Delta H^0(T \rightarrow G^-)$ will become smaller upon the amino ionization through $\Delta H^0_{hyd}(T \rightarrow G^-)$. The actual observation indeed meets this expectation, which indicates the parallelism between $\Delta H^0_{hyd}$ and $\Delta\mu^\dagger$.[28,29] In general, however, there is not a good correlation between $\Delta H^0$ and $\Delta\mu^\dagger$. This is due to the competition between the hydration and the intramolecular electrostatic interaction energies in the total enthalpy changes given by eq 2.

As done in the previous section to obtain $\Delta G^0_{hyd}(T \rightarrow G^+, G^-)$, $\Delta H^0_{hyd}(T \rightarrow G^+, G^-)$ is determined to be negative by adopting the ab initio results of $\Delta E^0_{gas}(T \rightarrow G^+, G^-)$ in eq 2. When the $-\Delta H^0_{hyd}$ values were plotted against $\Delta\mu^\dagger$, similar plots to those of $-\Delta G^0_{hyd}$ against $\Delta\mu^\dagger$ were obtained. This similarity is an indication of the dominance of $\Delta H^0_{hyd}$ in $\Delta G^0_{hyd}$. As $-\Delta H^0_{hyd}$ increases in trend with $\Delta\mu^\dagger$, it is concluded that a larger $\mu^\dagger$ reduces the conformer enthalpy to a larger extent through hydration.

In contrast to the conformational enthalpy change $\Delta H^0$, the entropy change $-T\Delta S^0$ can be assumed to be dominated simply by the hydration effect as

$$\Delta S^0 = \Delta S^0_{hyd} \tag{8}$$

Hence, we can expect a correlation between $-T\Delta S^0$ and $\Delta\mu^\dagger$. Here, the effect of changes in the solvent-accessible surface area (ASA) on the $-T\Delta S^0$ values can be neglected, as the changes in ASA associated with Asp and Asn side-chain conformational changes are estimated to be small, on the order of $10^{-1}$ to 1 Å$^2$. The $-T\Delta S^0$ value is plotted against $\Delta\mu^\dagger$ in Figure 6. All values appear in the first quadrant; the positive $-T\Delta S^0$ reflects the positive $\Delta\mu^\dagger$. This indicates that the stronger hydration due to $\mu^\dagger$ further restricts the freedom of the highly ordered water solvent. However, any correlation between $-T\Delta S^0$ and $\Delta\mu^\dagger$ was not seen.

The total conformational enthalpy $\Delta H^0$ and entropy $T\Delta S^0$ do not always compensate each other. For example, the transformation of conformer T to $G^+$ in Asp at neutral pD shows a positive enthalpy change and a negative entropy change. As it was shown above that $\Delta H^0_{hyd}$ and $T\Delta S^0_{hyd}$ have the same sign, the observed reinforcement between the total $\Delta H^0$ and $-T\Delta S^0$ is due to the effect of intramolecular electrostatic repulsion between α-$CO_2^-$ and $\beta$-$CO_2^-$, which is stronger than the effect of the hydration enthalpy. Thus, we show here a clear example of entropy−enthalpy noncompensation,[30] for which a microscopic interpretation is possible. Intramolecular electrostatic interaction, which competes with the hydration effect, plays a key role in breaking the compensation rule.

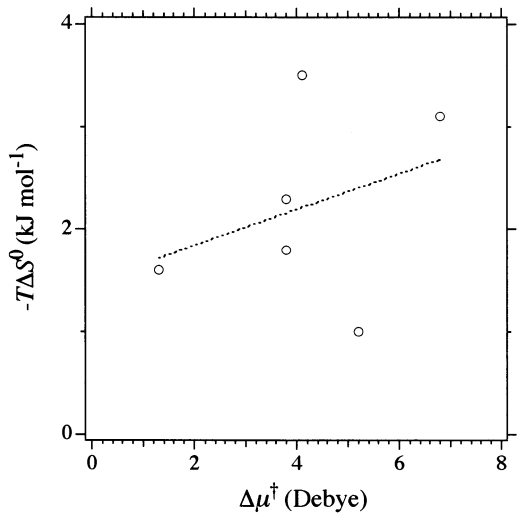


**Figure 6.** $-T\Delta S^0$ ($= -TS^0(G^+, G^-) + TS^0(T)$) against $\Delta\mu^\dagger$ ($= \mu^\dagger(G^+, G^-) - \mu^\dagger(T)$) for Asp. The dotted line represents the regression line obtained by the least-squares analysis.

In the case of aromatic side chains in tryptophan (Trp) and histidine (His) amino acids and peptides, there are reports of a good correlation between $\Delta H^0$ and $\Delta S^0$ in water-containing acidic or alkaline methanol solution; the solution pD and sequence positions of the residues were taken as the variables.[10,11] The intramolecular interactions in Trp and His are expected to be far weaker than the intramolecular charge−charge or charge−dipole interactions in Asp and Asn studied here. The compensation relation between $\Delta H^0$ and $-T\Delta S^0$ is expected to hold when both $\Delta H^0$ and $-T\Delta S^0$ are dominated simply by the hydration effect.

## 5. Conclusions

It has been accepted that the free-energy preference of the trans conformer for vicinal α-$CO_2^-$ and $\beta$-$CO_2^-$ in Asp ($\beta$-$CONH_2$ in Asn) is controlled by the intramolecular electrostatic repulsion between these groups. However, the ab initio results of $\Delta E^0_{gas}$ and the thermodynamic quantities experimentally obtained in this work were in disfavor of this view. It has been concluded that the hydration competes against the large intramolecular electrostatic repulsion, stabilizing the gauche conformers more than the trans. When the change $\Delta\mu^\dagger$ in the effective polarity is large, the overwhelming effect of hydration was observed for the enthalpy component. Only when $\Delta\mu^\dagger$ is small does the effect of intramolecular electrostatic repulsion become substantial. Because of the stronger hydration of the gauche conformers, the entropy of these conformers is smaller.

**Acknowledgment.** We are grateful for the support of this work by a Research Grant-in-Aid from the Ministry of Education, Science, and Culture (no.10304047). We thank Dr. Masahito Kubo of Kyoto University for insightful discussions.

## References and Notes


(1) Dill, K. A. *Biochemistry* **1990**, *29*, 7133.

(2) (a) Pachler, K. G. R. *Z. Anal. Chem.* **1967**, *39*, 211. (b) Taddei, F.; Pratt, L. *J. Chem. Soc.* **1964**, 1553. (c) Dale, B. J.; Jones, D. W. *Spectrochim. Acta, Part A* **1975**, *31*, 83.

(3) Bartle, K. D.; Jones, D. W.; L'Amie, R. *J. Chem. Soc., Perkin Trans. 2* **1972**, 650.

(4) Kainosho, M.; Ajisaka, K. *J. Am. Chem. Soc.* **1975**, *97*, 5630.

(5) Sealy, R. C.; Harman, L.; West, P. R.; Mason, R. P. *J. Am. Chem. Soc.* **1985**, *107*, 3401.

(6) (a) Bystrov, V. F. *Prog. Nucl. Magn. Reson. Spectrosc.* **1976**, *10*, 41. (b) Wüthrich, K. *NMR of Proteins and Nucleic Acids*; Wiley & Sons: New York, 1986.

(7) Cavanaugh, J. R. *J. Am. Chem. Soc.* **1970**, *92*, 1488.

(8) Wyssbrod, H, R.; Ballardin, A.; Schwartz, I. L.; Walter, R.; Binst, G. V.; Gibbons, W. A.; Agosta, W. C.; Field, F. H.; Cowburn, D. *J. Am. Chem. Soc.* **1977**, *99*, 5273.

(9) Kobayashi, J.; Higashijima, T.; Nagai, U.; Miyazawa, T. *Biochim. Biophys. Acta* **1980**, *621*, 190.

(10) Jäckle, H.; Luisi, P. L. *Biopolymers* **1981**, *20*, 65.

(11) Baici, A.; Rizzo, V.; Skrabal, P.; Luisi, P. L. *J. Am. Chem. Soc.* **1979**, *101*, 5170.

(12) (a) Karplus, M. *J. Chem. Phys.* **1959**, *30*, 11. (b) Karplus, M. *J. Am. Chem. Soc.* **1963**, *85*, 2870.

(13) Pople, J. A.; Schneider, W. G.; Bernstein, H. J. *High-Resolution Nuclear Magnetic Resonance*; McGraw-Hill: New York, 1959.

(14) Pachler, K. G. R. *Spectrochim. Acta* **1964**, *20*, 581.

(15) (a) Glick, R. E.; Bothner-By, A. A. *J. Chem. Phys.* **1956**, *25*, 362. (b) Sheppard, N.; Turner, J. J. *Proc. R. Soc. London, Ser. A* **1959**, *252*, 506. (c) Abraham, R. J.; Pachler, K. G. R. *Mol. Phys.* **1963**, *7*, 165.

(16) (a) Williams, D. H.; Bhacca, N. S. *J. Am. Chem. Soc.* **1964**, *86*, 2742. (b) Booth, H. *Tetrahedron Lett.* **1965**, 411.

(17) Feeney, J. *J. Magn. Reson.* **1976**, *21*, 473.

(18) Glasoe, P. K.; Long, F. A. *J. Phys. Chem.* **1960**, *64*, 188.

(19) (a) Huzinaga, S. *J. Chem. Phys.* **1965**, *42*, 1293. (b) Dunning, T. H. *J. Chem. Phys.* **1970**, 53, 2823.

(20) Schmidt, M. W.; Baldridge, K. K.; Boatz, J. A.; Elbert, S. T.; Gordon, M. S.; Jensen, J. H.; Koseki, S.; Matsunaga, N.; Nguyen, K. A.; Su, S. J.; Windus, T. L.; Dupuis, M.; Montgomery, J. A. *J. Comput. Chem.* **1993**, *14*, 1347.

(21) Ding, Y.; Krogh-Jespersen, K. *Chem. Phys. Lett.* **1992**, *199*, 261.

(22) Yu, D.; Armstrong, D. A.; Rauk, A. *Can. J. Chem.* **1992**, *70*, 1762.

(23) Langlet, J.; Caillet, J.; Evleth, E.; Kassab, E. Modeling of Molecular Structures and Properties. In *Studies in Physical and Theoretical Chemistry*; Rivail, J.-L., Ed.; Elsevier: Amsterdam, 1990; Vol. 71, p 345.

(24) $\Delta E^0_{gas}(T \rightarrow G^+)$ for the ionization state of neutral pH could not be calculated because of the hydrogen transfer from α-$NH_3^+$ to α-$CO_2^-$ in the optimization for conformer $G^+$. Energy calculations with the MM2 force field[25] for this ionization state provided $\Delta E^0_{gas}(T \rightarrow G^+)$ and $\Delta E^0_{gas}(T \rightarrow G^-)$ values of 128.4 and 49.8 kJ $mol^{-1}$, respectively.

(25) Burkert, U.; Allinger, N. L. *Molecular Mechanics*; American Chemical Society: Washington, DC, 1982.

(26) The semiempirical AM1 calculation[27] provided a $\mu^\dagger$ value of 13.9 D for conformer $G^+$ at the ionization state of the neutral pH.

(27) Dewar, M. J. S.; Zoebisch, E. G.; Healy, E. F.; Stewart, J. J. P. *J. Am. Chem. Soc.* **1985**, *107*, 3902.

(28) On the transformation from T to $G^-$, the β-carboxylate group remains gauche to the α-amino/ammonium group. Therefore, we can neglect the effect of their ionization-state-dependent intramolecular electrostatic interaction on $\Delta H^0$. For the transformation from T to $G^+$, the ionization of the amino group contributes to the increase of $\Delta H^0$ due to the increased attraction with the β-carboxylate group. The observed decrease of $\Delta H^0$ indicates the overwhelming hydration effect.

(29) We see the $\Delta G^0_{hyd} - \Delta\mu^\dagger$ correlation at the same time by also taking account of the entropy term $-T\Delta S^0$ because we can assume that $\Delta S^0 = \Delta S^0_{hyd}$ as represented in eq 8 and observe that $-T\Delta S^0$ reflects the trend of $\Delta\mu^\dagger$.

(30) Gallicchio, E.; Kubo, M. M.; Levy, R. M. *J. Am. Chem. Soc.* **1998**, *120*, 4526.